



AMERICAN METEOROLOGICAL SOCIETY

Journal of the Atmospheric Sciences

EARLY ONLINE RELEASE

This is a preliminary PDF of the author-produced manuscript that has been peer-reviewed and accepted for publication. Since it is being posted so soon after acceptance, it has not yet been copyedited, formatted, or processed by AMS Publications. This preliminary version of the manuscript may be downloaded, distributed, and cited, but please be aware that there will be visual differences and possibly some content differences between this version and the final published version.

The DOI for this manuscript is doi: 10.1175/JAS-D-16-0325.1

The final published version of this manuscript will replace the preliminary version at the above DOI once it is available.

If you would like to cite this EOR in a separate work, please use the following full citation:

Dandu, G., B. Vadlamudi, and A. Karumuri, 2017: Understanding the Revival of the Indian Summer Monsoon after Breaks. *J. Atmos. Sci.* doi:10.1175/JAS-D-16-0325.1, in press.



1 **Understanding the Revival of the Indian Summer Monsoon after Breaks**

2

3

4 Govardhan Dandu¹, Vadlamudi Brahmananda Rao² and Karumuri Ashok¹

5

6 1. University Centre for Earth and Space Sciences, University of Hyderabad, Hyderabad.

7 2. Emeritus professor, INPE, Brazil.

8

9

10 Corresponding Author: Karumuri Ashok, Center for Earth and Space Sciences,

11 University of Hyderabad, Hyderabad, 500046, India. (ashokkarumuri@uohyd.ac.in)

12

13

14

15

16

17

18

19

20

21

22

23

24

25

26

PRELIMINARY ACCEPTED VERSION

27 **ABSTRACT**

28

29 In this paper, we suggest a dynamical mechanism involved in the revival of summer monsoon after
30 breaks. In this context, we carry out a diagnostic analysis using the datasets from National Centres
31 for Environmental Prediction reanalysis-II for the period 1979-2007 to identify a robust mechanism
32 that typifies breaks and subsequent revival of monsoon. We find that during the peak of significant
33 breaks, an anomalous southward shift of subtropical westerly jet stream, which is invariably
34 accompanied by anomalous northward shift of a stronger-than-normal easterly jet. These major
35 changes during a break facilitate an instability mechanism, which apparently leads to formation of a
36 synoptic disturbance. Formation of such a disturbance is critical to the subsequent revival of
37 summer monsoon in 61% of the observed break to active revivals.

38 Computations of energetics and correlation analysis carried out suggest an increase in the eddy
39 kinetic energy at the expense of the mean kinetic energy during the breaks, in agreement with the
40 formation of the synoptic disturbance. This demonstrates that barotropic instability in the presence
41 of a monsoon basic flow is the primary physical mechanism that controls the revival of the summer
42 monsoon subsequent to the break events.

43

44

45

46

47

48 Key words: Barotropic instability; Indian summer monsoon; monsoon breaks

49

50

51

52

53 **1. INTRODUCTION**

54

55 The spatial and temporal variability of during the Indian summer monsoon (ISM) is very important
56 for a country like India, which is mainly based on agriculture. The ISM experiences, in addition to
57 the dominant interannual variability, intraseasonal variability in the form of active and break spells
58 of rainfall. Blanford (1886), in a pioneering work suggested the “intervals of drought” as the break
59 periods during the peak monsoon months of July-August. Also, recent studies suggest that droughts
60 are associated with longer breaks (Joseph et al. 2009, Raman and Rao 1981). Typically, during the
61 monsoon breaks, the monsoon trough in the sea level pressure, normally extending from the Head
62 Bay of Bengal northwestward into Gujarat and adjoining Pakistan, is seen to propagate further north
63 into the foothills of Himalayas. This results in anomalously surplus rainfall in the Himalayan
64 regions, and below normal rainfall to the south (Ramamurthy 1969, Krishnamurti and Ardanuy
65 1980, Krishnan et al. 2000, 2009, Rajeevan et al. 2008, 2010). The active condition of the ISM, on
66 the other hand, is when the sea level pressure trough moves south of its normal position, resulting in
67 above normal rainfall along the climatological monsoon trough regions and in many places of the
68 peninsular (Sikka and Narsimha 1995, Rao 1976, Alexander et al. 1978, Das 2002, Rajeevan et al.
69 2010, Choudhury and Krishnan 2011). Compared with other scales intraseasonal variability of the
70 ISM represents higher amplitude of the seasonal mean (Goswami 2011, Waliser 2006). Goswami
71 (2003) suggest that emphasis of meridional shear of zonal winds and cyclonic vorticity along the
72 monsoon trough results in increased (decreased) frequency of occurrence of low pressure systems
73 during active (break) phase by the intraseasonal oscillations. The intraseasonal variability of ISM
74 manifests as two broad peaks of variability, namely a 10-20 day and a 30-60 day variability, with
75 active and break phases which are linked to the northward migration of monsoon trough/ridge (Pai
76 et al. 2009, Krishnamurti and Subrahmanayam 1982, Joseph and Sijikumar 2004, Krishnamurti and
77 Shukla 2007).

78 The revival of active conditions during the ISM is facilitated by the formation of synoptic
79 disturbances in the Bay of Bengal, monsoon depressions and low pressure systems that travel
80 towards the northwest from Bay of Bengal into the Indian region (Chen et al. 2005, Sikka & Dixit
81 1972, Boos et al. 2015, Sikka & Gadgil 1980), many a times along the monsoon trough, and cause
82 copious rainfall. Krishnamurthy and Ajayamohan (2010) have shown that the absence of low
83 pressure systems such as lows, depressions, cyclonic storms etc., represents the break phase and
84 its presence concluded as active phase of ISM.

85

86 From a dynamical perspective, some pioneering papers by Ramaswamy (1956, 1962) highlight the
87 importance of anomalous southward shift of large-amplitude westerly troughs from the mid-
88 latitudes into the Indo-Pakistan region during breaks in the ISM. Importantly, further analysing a
89 case study studied by Ramaswamy (1962), Rao (1971) documents a manifestation of barotropic
90 instability associated with increased horizontal shear due to the southward shift of the westerly
91 troughs in the subtropical westerly jet at mid-tropospheric level in the aforementioned break event,
92 and a subsequent revival associated with the formation of a synoptic disturbance. Rao (1971)
93 hypothesized that manifestation of the barotropic instability during break leads to the formation of
94 disturbances, which in turn invigorate the ISM an active phase. Satyan et al. (1980) addressed the
95 problem by using a two-layer quasigeostrophic model and carried out a stability analysis of the
96 simulated monsoon zonal flow corresponding to break conditions, and in this work, Satyan et al.
97 also document the revival of the post-break monsoon through formation of a synoptic disturbance.
98 Further, while the upper level flow in the simulations of Satyan et al. (1980) is found to be stable
99 during the break monsoon conditions, it was found to be unstable a day before the formation of
100 depression, supporting the argument of Rao (1971).

101 In the next few sentences, we briefly discuss some of the possible mechanisms such as the
102 barotropic, baroclinic instabilities and other combined mechanisms, which have been suggested to
103 explain the growth of the synoptic disturbances. The combined barotropic-baroclinic wind field

104 study of the monsoon by Shukla (1977); using a ten layered quasi-geostrophic model, found that the
105 barotropic mode is the only source for the upper tropospheric growing mode at 150 hPa. Shukla
106 (1978) numerically integrated the linearized perturbation equations for a three-layer
107 quasigeostrophic model and performed a combined CISK-barotropic-baroclinic instability analysis,
108 which shows the maximum growth rate occurs for the smallest scales. On the other hand, Goswami
109 (1980), while suggesting that a large meridional shear of the eastward component of winds at 200
110 hPa level and a high cyclonic vorticity at low levels over the monsoon trough region during break
111 periods favour growth of barotropic and baroclinic instabilities, adds that these instabilities cannot
112 explain the initial growth for monsoon depressions. Therefore, the question remains whether
113 instabilities generated by large scale processes lead to subsequent revival of the monsoon through a
114 barotropic instability mechanism and formation of a synoptic disturbance. In this paper, we attempt
115 to answer this question. The availability of reanalysis datasets in the recent decades is a great
116 opportunity in this sense. Analysis of multiple cases will also help us to refine any theoretically-
117 based thresholds and indices that represent a phenomenon. For example, theory (Kuo 1953, Starr &
118 White, 1954, Aihara 1959) suggests that barotropic instability occurs only in disturbances of very
119 long wavelengths. The case study of a break monsoon Rao (1971) suggests that synoptic waves in
120 subtropical westerly jet in the Indian region with a wavelength of above (below) 3,000 km are
121 unstable (stable). We revisit this aspect in this study. The details of the datasets used and methods
122 of analysis are described in the next section. We present our results in section3, followed by a
123 section on the conclusions and discussion.

124

125 **2. DATA AND METHODS**

126 *2. a. Data*

127

128 For the present study, we have used break monsoon periods based on Rajeevan et al. (2008) of ISM
129 for the period 1979-2007. Following Rajeevan et al. (2010), we choose the region bounded by from

130 18.0° N to 28.0° N and 65.0° E to 88.0° E as the core monsoon region; indeed, on inter-annual
 131 scale, the area-averaged rainfall in this region is highly correlated at 0.91 with that of inter-annual
 132 variation of the Indian summer monsoon, (Rajeevan et al. 2010). The daily data employed in the
 133 study are zonal (U) wind at 200 hPa, Meridional (V) wind, Geopotential Height and Sea level
 134 pressure (SLP). All of these products were obtained from National Centres for Environmental
 135 Prediction (NCEP) reanalysis 2 (Kanamitsu et al. 2002). These Datasets are of spatial resolution
 136 2.5° lat x 2.5° long global grid and temporal coverage are 4-times daily values for 1979/01/01 to
 137 2007/12/31. In addition, the dates of the synoptic disturbances and locations were collected from the
 138 IMD (Cyclone eAtlas) data. In addition, the sea level pressure (SLP) data from the NCEP
 139 reanalysis 2 data were used to reconfirm the dates of formation of the synoptic disturbances. We
 140 adopt the breaks and active event dates following Rajeevan et al. (2010).

141

142 2. b. *Method*

143

144 Following Kuo (1953), Syono & Aihara, (1957) and Rao (1971), an index for barotropic instability
 145 is defined as the meridional shear in the daily 200 hPa zonal wind. Further, the critical wavelength
 146 (neutral wavelength) of a zonal wave at this level is computed as

$$147 \quad L_c = \frac{2D}{\sqrt{3}} \quad (1)$$

148 Where D/2 is the zonal width between subtropical westerly jet and tropical easterly jet. Indeed,
 149 Waves longer than L_c (wavelength) become unstable and below L_c are stable (Starr & White, 1954;
 150 Aihara, 1959). The rate of Conversion of Mean Kinetic Energy (CMKE) is obtained by

151

$$152 \quad C(\bar{K}, K') = \int U \frac{\partial}{\partial y} \bar{v' u'} dm \quad (2)$$

153

154 Where m is the mass, \bar{K} is the Mean kinetic energy (Joule/sec), K' is the Eddy kinetic energy, U is
 155 the zonal wind (m/s) and V is the meridional wind (m/s). A complete list of the symbols/notations

156 representing various variables/parameters in this study is provided in Table 1. The u' and v' have
 157 been obtained as the daily anomalies from the zonal mean of the respective circulation component
 158 averaged over 20° E and 120° E. Equation 2 means that if there is divergence (convergence) of
 159 eddy momentum transport in region of westerlies, \bar{K} gets converted into $K'(K'$ gets converted into
 160 \bar{K}), that is, the disturbance is barotropically unstable (stable). In our analysis, we use the criterion
 161 by Kuo (1951), which states that, for barotropic instability to happen at a location, the meridional
 162 gradient of the absolute vorticity has to be either maximum or minimum. The corresponding
 163 mathematical expression is shown in the equation 3.

164

165
$$\frac{d\zeta}{dy} = 0$$

166 As per Kuo (1951) the above expression for the largely zonal flow can be approximated as,

167
$$\frac{d}{dy} \left(\frac{-d\bar{U}}{dy} + f \right) = 0 \quad (3)$$

168 Where \bar{U} is the mean zonal wind, f is the Coriolis force and ζ is the absolute vorticity. We
 169 use the criterion shown in equation (3) to explain the mechanism behind the formation of the post-
 170 break synoptic disturbances over the Indian region and the Bay of Bengal, which reactivate the
 171 Indian summer monsoon.

172

173 **3. RESULTS AND DISCUSSION**

174 ***3. a. Barotropic instability in the aftermath of breaks***

175

176 From the works of Starr and White (1954) and Rao (1971), we can suppose that such a break
 177 condition will result in barotropic instability, which may *in turn* manifest as a synoptic disturbance
 178 for the revival of ISM. In this context, from the Table 1, following Rajeevan et al. (2008), we list
 179 the dates of various post-break revival events of ISM. Of the 41 total events (Table 2), 18 revivals
 180 occurred with formation of a low pressure in the Bay of Bengal (Fig. 1, shown as an example), and

181 7 others with formation of a low pressure on land (Figures not shown). This result suggests that
 182 about 61% of the post break revivals are associated with formation of a low pressure in the Bay of
 183 Bengal or land regions, providing a general support to the hypothesis of Rao (1971) and Raghavan
 184 (1973).

185

186 Now, eddy formation due to barotropic instability would necessitate a conversion of the \bar{K} into K' ,
 187 as shown by the equation 2. Indeed, this is true in many 30 out of the 41 cases i.e. 73% of post-
 188 break revival events, as evidenced by the positive values of CMKE (Table 3) (Fig. 2). This indicates
 189 that the barotropic instability is the primary possible large scale dynamical instability mechanism
 190 during the ISM breaks, and many times leading to formation of synoptic eddies. Another way to
 191 ascertain this further is by checking that there exists a significant negative correlation between the
 192 CMKE and wavelength, an indication of barotropic instability (e.g. Rao, 1971). We find a strong
 193 correlation of -0.285 (Table 2), which is significant at 95% confidence level from a Student's two
 194 tailed test. This significant correlation confirms that barotropic instability is indeed manifested after
 195 the break monsoon events, and is a necessary condition for the revival of Indian Summer Monsoon
 196 after break conditions.

197

198 What is the potential mechanism for such manifestation of barotropic instability in these sub-
 199 seasonal events? As known, barotropic disturbances derive energy from the mean kinetic energy.
 200 Energy considerations (e.g. Kuo 1951) show that for a disturbance to grow, it must tilt in a direction
 201 opposite to that of the meridional gradient of zonal wind. To be specific, a tilt from Southwest to
 202 Northeast (SW-NE) in a westerly zonal flow will meet this criterion. That is, waves with a tilt from
 203 the SW-NE will result in a maximum vorticity to the south (see equation 3, which is from Kuo
 204 1949). From supplementary figures S1 & S2, it is seen most of the break days are also indeed
 205 associated with such a SW-NE tilt in the 200 hPa zonal flow. Such a tilt in the mean 200 hPa
 206 subtropical westerly jet over the Indian region on a typical break day, shown in Fig. 3a as well as

example, along with the corresponding geopotential field (Fig. 3b), is associated with a northward transfer of westerly momentum (Kuo, 1949). In such a case, the zonally averaged eddy momentum transport ($\overline{u'v'}$) will be positive, and is, importantly, conducive to the formation of an eddy disturbance (Fig. 4a) associated with maximum vorticity to its south (Kuo, 1949). Truly, the corresponding zonal wind structure at 200 hPa shows a southward shift of the westerly jet during the break period and a northward shift of the tropical easterly jet (Fig. 4b).

213

From the point of Rao (1971), it will be instructive to verify that the barotropic instability is a mechanism that would help the aforementioned eddies grow in such situations. To that end, the meridional vorticity distribution of the absolute vorticity ζ in the Indian region during the break events are presented in Fig. 5a, along with the corresponding composite in Fig. 5b. Importantly, we see maximum or minimum in absolute vorticity ζ around 29° N in the composite, with the individual values varying between 25° to 30° N. Manifestation of such maximum or minimum values is a necessary condition for the barotropic instability (Kuo, 1951) from the individual case also indicates such manifestation (Fig. 5b). All this highlights the importance of the mean seasonal zonal wind structure, with westerlies to the north and easterlies to the south of the Indian sub-continent, in facilitating such a dynamical instability manifested by the breaks.

224

225 ***3. b. Wavelength Threshold for manifestation of a post-break synoptic disturbance***

226

227 Ramaswamy (1962) & Rao (1971), claim from their individual case studies, a decrease in channel
 228 width ($D/2$) between subtropical westerly and tropical easterly jets that manifest as a dynamical
 229 instability. We revisit this aspect by computing the $D/2$ during the break events in the study period.
 230 Our results, shown in Tables 4, Fig. 6, show that 32 out of 41 break events (78 %) indeed show a
 231 decrease in channel width. From this, we can deduce that a dynamical instability during the breaks
 232 is facilitated either due to a transient southward shift of the westerlies over the northern portions of

233 the subcontinent and/or a transient northward shift of the tropical easterly jet stream over the
 234 peninsular region. Such a decrease in the channel width in the zonal width can also manifest with a
 235 weakening (strengthening) of the upper level westerlies (easterlies) in the Indian region.

236

237 Theory (Kuo 1953, Syono & Aihara 1957) shows that barotropic instability occurs only in zonal
 238 waves of wavelength shorter than a critical wavelength L_c (see Equation 1). Rao (1971), from his
 239 sole case study, estimates L_c of the upper level westerly Jetstream in the Indian region to be the
 240 ~3000 km. However, given that it was only a single case, and the relatively poor quality of the
 241 upper air data during that period, we use the reanalysed gridded datasets for multiple break
 242 monsoon cases to revisit this important finding by Rao (1971). Our analysis using equation 1(Table
 243 4) shows that (i) wavelengths in the upper level westerlies north of Indian region during the summer
 244 monsoon season reach a minimum value during breaks as compared to a few days prior and after
 245 the event, and (ii) The critical mean critical value of the aforementioned wavelength, obtained by
 246 averaging it over all break events, comes to 7411 km. The minimum L_c we find is just 5127 km
 247 (Fig. 7; also see Table 5).

248

249 **4. CONCLUSIONS**

250 Ramaswamy (1962) and Rao (1971) show, through individual case studies that transition from
 251 break to active conditions occurs during the Indian summer monsoons (ISM) owing to the
 252 manifestation of barotropic instability, which leads to formation of a synoptic disturbance. Given
 253 the critical importance of break-active cycles in defining the seasonal rainfall envelope (Goswami
 254 2003 or Goswami and Ajayamohan 2001) during the ISM, it is very important to revisit the
 255 conclusions of these case studies. With this goal in mind, using the atmospheric circulation datasets
 256 from the NCEP-NCAR reanalysis II (Kanamitsu et al. 2002) for the period 1979-2007, we explore
 257 the potential role of break-monsoon conditions in subsequent revival of the monsoons through
 258 formation of a synoptic disturbance in the Indian region. We adopt the active and break monsoon

259 calendar documented by Rajeevan et al. (2008). We find that barotropic instability manifests in the
260 Indian region during break monsoons in 61% of the cases. Such a revival is found to be associated
261 with a reduction of the ‘zonal width’ between the upper level subtropical westerlies and tropical
262 easterlies. Our correlation analysis between the wave length of zonal winds in the Indian region and
263 rate of conversion of mean kinetic energy values for the study period is -0.285, statistically
264 significant at 95% confidence level, which confirms the role of barotropic instability for formation
265 of the post-break synoptic disturbance (e.g. Aihara 1959). During the break monsoon period over
266 most of the country there is no rainfall, and therefore the succeeding disturbances are not generated
267 by the condensation heating. Thus, the argument that generation of monsoon depressions and
268 synoptic disturbances due to the break-induced barotropic instability is reasonable. We also find
269 that the mean wavelength of westerlies during boreal monsoon events north of the Indian region,
270 which leads to the revival of the monsoons, is about 7400 km. While Rao (1971) suggests a
271 threshold wavelength of 3,000 km from his study, our analysis of the 41 cases suggests an apparent
272 threshold from our sample to be above 5,000 km.

273

274 As this study has been mainly carried out using the NCEP-NCAR reanalysis II (Kanamitsu et al.,
275 2002), in future, we plan to explore these issues in other reanalysis data and various available
276 medium range hindcast runs (e.g. Mitra 2003, 2009, 2013), and by conducting a few numerical
277 sensitivity experiments.

278 We also need to remember that the Indian summer monsoon variability is controlled by several
279 factors and drivers. In addition, formation of a disturbance depends on various other factors such as
280 the SST, moisture availability, etc. The monsoon can also revive due to large scale circulation
281 changes, in which case the manifested instability may be different. From this context, the relevance
282 of the other mechanisms, such as the baroclinic instability, in the remaining cases of the break-
283 active transitions that happen without the formation of a synoptic disturbance needs further
284 examination.

285

286 **Acknowledgments**

287

288 The authors gratefully acknowledge the Indian Meteorological Department (IMD), India, for the
 289 cyclone/synoptic disturbance chronology (eAtlas) data from www.rmcchennaieatlas.tn.nic.in, and
 290 the NOAA-Earth System Research Laboratory (ESRL), The Climate Diagnostics Center, USA, for
 291 providing the National Centers for Environmental Prediction (NCEP II reanalysis) data from
 292 www.esrl.noaa.gov/psd/data/gridded/data.ncep.reanalysis2.html

293

294

295

296

297 **Appendix-I**

298

299 These are two ways of studying the development of disturbances, namely,

300 1. Eigen value problem (Dynamic Meteorology by Holton)
 301 2. The initial value problem (Kuo 1953; also see Chapter 6 of Krishnamurti, 2013)

302 Here we have adopted the initial value problem. The symbols/notations representing various
 303 variables/parameters in the appendix are listed below (Table A1).

304

305 In order to estimate the energy exchange between the basic zonal current and a superimposed
 306 disturbance in a barotropic, non-divergent and frictionless atmosphere, we use the barotropic
 307 vorticity equation in the form.

308

309

310
$$\frac{d}{dt}(f + v_E) = 0 \quad (1)$$

311 where

312
$$\frac{d}{dt} = \frac{\partial}{\partial t} + u \frac{\partial}{\partial x} + v \frac{\partial}{\partial y}$$

313

314 $f = 2\Omega \sin(\phi)$; Coriolis force term

315 ϕ - Latitude

316 $\nu_E = \nabla^2 \psi$ - Relative vorticity

317 ψ - Stream function

318 u and v are the zonal and meridional components of the horizontal velocity vector, and can be

319 expressed as

320 $u = \frac{-\partial \psi}{\partial y}; v = \frac{\partial \psi}{\partial x}$

321

322 As can be understood, x & y are the co-ordinate axes taken positive towards east and north
323 respectively.

324 Linearization of equation (1) yields

325

326
$$\frac{\partial}{\partial t} \nabla^2 \psi + U \frac{\partial}{\partial x} \nabla^2 \psi + \frac{\partial \psi}{\partial x} \left(\beta - \frac{\partial^2 U}{\partial y^2} \right) = 0 \quad (2)$$

327 U is the mean zonal current and ψ is the stream function for the perturbation flow.

328 $\beta = \frac{df}{dy}$ --- Rossby factor

329 A typical solution for equation (2) will be

330

331 $\psi = A(y, t) \sin(kx) + B(y, t) \cos(kx) \quad (3)$

332 Where $k = \frac{2\pi}{L}$ is the wave number, and L the Wavelength

333 Substituting solution (3) in the equation (2) and equating the coefficients of Sin (kx) and Cos (kx)
334 terms, we get the following equations:

335

336
$$\frac{\partial^2}{\partial y^2} \left(\frac{\partial A}{\partial t} \right) - k^2 \frac{\partial A}{\partial t} = -U \left(k^3 B - K \frac{\partial^2 B}{\partial y^2} \right) + k B \left(\beta - \frac{\partial^2 U}{\partial y^2} \right) \quad (4)$$

337

338
$$\frac{\partial^2}{\partial y^2} \left(\frac{\partial B}{\partial t} \right) - k^2 \frac{\partial B}{\partial t} = U \left(k^3 A - K \frac{\partial^2 A}{\partial y^2} \right) - k A \left(\beta - \frac{\partial^2 U}{\partial y^2} \right) \quad (5)$$

339

340

341 (4) and (5) are two unknown equations in two unknowns, $\frac{\partial A}{\partial t}$ and $\frac{\partial B}{\partial t}$ and so form a closed system of
 342 equations.

343

344 From the prescribed initial values of u , A , B , and $\frac{\partial^2 U}{\partial y^2}$, and with proper boundary conditions, we
 345 can find solutions for $\frac{\partial A}{\partial t}$ and $\frac{\partial B}{\partial t}$.

346

347 **Initial conditions**

348

349 $A_o=0$ and $B_o=a \sin y$, $l = \frac{\pi}{D}$ (6)

350 where D is the channel width, and suffix 'o' represents the initial value . As pointed by Platzman
 351 (1952), it is desirable to take initial conditions in such a way as to make the first derivative of
 352 perturbations kinetic energy zero. As would be shown later specifically in equation (10), the above
 353 condition (6) will fulfil the requirement.

354

355 **Boundary conditions-- Meridional direction**

356

357 $A=0$ at $y=0$ and $y=D$; $\frac{\partial A}{\partial t}=0$ and $\frac{\partial B}{\partial t}=0$ at $y=0$ and $y=D$ (7)

358

359 In the X-direction we assume that the disturbance quantities have cyclic periodicity at intervals of
 360 one wavelength L. If Q is any disturbance quantity, then $Q(x,y)=Q(x\pm L,y)$. Thus it is sufficient to
 361 consider the domain of integration as the area bounded by one wavelength 'L' in the X- direction
 362 and distance D in the y- direction to evaluate various kinds of energies.

363

364 **Time tendency of Amplitudes**

365

366 Amplitudes A and B after a time Δt are given by the Taylor's series

367

368
$$A(\Delta t) = A_o + \left(\frac{\partial A}{\partial t}\right)_o \Delta t + \frac{1}{2} \left(\frac{\partial^2 A}{\partial t^2}\right)_o \Delta t^2 \pm \dots \quad (8)$$

369

370

371
$$B(\Delta t) = B_o + \left(\frac{\partial B}{\partial t}\right)_o \Delta t + \frac{1}{2} \left(\frac{\partial^2 B}{\partial t^2}\right)_o \Delta t^2 \pm \dots \quad (9)$$

372

373 If Δt is sufficiently small, the above series can be truncated after the second derivative. This will no
 374 doubt introduce some error in the forecasted amplitudes. Nevertheless, it is not an essential
 375 shortcoming as shown by the results.

376 With initial conditions (6), (5) becomes

377

378
$$\frac{\partial^2}{\partial y^2} \left(\frac{\partial B}{\partial t}\right) - k^2 \left(\frac{\partial B}{\partial t}\right) = 0 \quad (10)$$

379

380 It can easily be shown from (10) and (7) that $\left(\frac{\partial B}{\partial t}\right)_o = 0$, everywhere,

381 Equations for $\left(\frac{\partial^2 A}{\partial t^2}\right)_o$ and $\left(\frac{\partial^2 B}{\partial t^2}\right)_o$ can be obtained by differentiating (4) and (5) with respect to time.

382 They take the form

383

384
$$\frac{\partial^2}{\partial y^2} \left(\frac{\partial^2 A}{\partial t^2} \right) - k^2 \frac{\partial^2 A}{\partial t^2} = -U \left(k^3 \frac{\partial B}{\partial t} - K \frac{\partial^2}{\partial y^2} \left(\frac{\partial B}{\partial t} \right) \right) + k \frac{\partial B}{\partial t} \left(\beta - \frac{\partial^2 U}{\partial y^2} \right) \quad (11)$$

385

386
$$\frac{\partial^2}{\partial y^2} \left(\frac{\partial^2 B}{\partial t^2} \right) - k^2 \frac{\partial^2 B}{\partial t^2} = U \left(k^3 \frac{\partial A}{\partial t} - K \frac{\partial^2}{\partial y^2} \left(\frac{\partial A}{\partial t} \right) \right) - k \frac{\partial A}{\partial t} \left(\beta - \frac{\partial^2 U}{\partial y^2} \right) \quad (12)$$

387

388 Initial conditions (6) are used to obtain (11) and (12) since $\left(\frac{\partial B}{\partial t} \right)_0 = 0$ from equations (11) and (7)

389 it can easily be shown that $\left(\frac{\partial^2 A}{\partial t^2} \right)_0 = 0$ everywhere, so (8) and (9) reduce to

390

391
$$A(\Delta t) = \left(\frac{\partial A}{\partial t} \right)_0 \Delta t \quad (13)$$

392

393
$$B(\Delta t) = B_0 + \frac{1}{2} \left(\frac{\partial^2 B}{\partial t^2} \right)_0 \Delta t^2 \quad (14)$$

394

395 so after time Δt , ψ is given by

396

397
$$\psi(\Delta t) = A(\Delta t) \sin(kx) + B(\Delta t) \cos(kx)$$

398

399
$$\psi(\Delta t) = R_\psi \cos(kx - \delta\psi) \quad \text{where } R_\psi = [A^2(\Delta t) + B^2(\Delta t)]^{1/2}$$

400

401 and $\tan(\delta\psi) = \frac{A(\Delta t)}{B(\Delta t)}$ (15)

402

403 Thus the amplitude and phase of ψ wave can be found after time Δt from (15)

404

405 **Initial change of kinetic energy**

406

407 The rate of change of kinetic energy may be regarded as the rate of amplification of the
 408 disturbances. If it is positive, kinetic energy tends to increase with time, and disturbance is said to
 409 be unstable. If it is negative, kinetic energy tends to decrease, and the disturbance is said to be
 410 stable or damping. If the rate of change of kinetic energy is zero, the kinetic energy remains
 411 constant, and the disturbance is said to be neutral.

412

413 The kinetic energy of the disturbance is given by

414

$$415 \quad K_r = \int_0^D \int_0^L \frac{u^2 + v^2}{2} dx dy \quad (16)$$

416

417 But

$$418 \quad u = \frac{-\partial \psi}{\partial y} = - \left[\frac{\partial A}{\partial y} \sin(kx) + \frac{\partial B}{\partial y} \cos(kx) \right] \quad (17)$$

419

$$420 \quad v = \frac{\partial \psi}{\partial x} = -k[A \cos(kx) - B \sin(kx)] \quad (18)$$

421

422 Inserting (17) and (18) into (16) we get

423

$$424 \quad K_r = \frac{\pi}{2k} \int_0^D \left[\left(\frac{\partial A}{\partial y} \right)^2 + \left(\frac{\partial B}{\partial y} \right)^2 + k^2(A^2 + B^2) \right] dy \quad (19)$$

425

426 Differentiating (19) with respect to time and using (4), (5) and (7) we get

427

$$428 \quad \frac{\partial K_r}{\partial t} = -\pi \int_0^D U \left[A \frac{\partial^2 B}{\partial y^2} - B \frac{\partial^2 A}{\partial y^2} \right] dy \quad (20)$$

429

430 The equation for the time change of the zonal wind is

431

432
$$\frac{\partial U}{\partial t} = \frac{-\partial}{\partial y} \bar{u}\bar{v} \quad (21)$$

433 where the overbar denotes a zonal average.

434 Multiplying (21) by U and integrating over the region we get the equation for the time change of
435 zonal kinetic energy as

436

437
$$\frac{\partial}{\partial t} K_{r_z} = - \int_0^D \int_0^L U \frac{\partial}{\partial y} \bar{u}\bar{v} dx dy \quad (22)$$

438

439 Where K_{r_z} is the zonal kinetic energy given by

440

441
$$K_{r_z} = - \int_0^D \int_0^L \left(\frac{U^2}{2} \right) dx dy$$

442

443 Using (17) and (18)

444

445
$$\bar{u}\bar{v} = \frac{k}{2} \left[B \frac{\partial A}{\partial y} - A \frac{\partial B}{\partial y} \right] \quad (23)$$

446

447 Using (23) and (22) becomes

448

449
$$\frac{\partial}{\partial t} K_{r_z} = \pi \int_0^D U \left[A \frac{\partial^2 B}{\partial y^2} - B \frac{\partial^2 A}{\partial y^2} \right] dy \quad (24)$$

450

451 It is seen from (20) and (24) that the right hand side of (24) is the same as the right hand side of (20)
452 but with opposite sign. Thus this term represents the interaction between the zonal and perturbation
453 kinetic energies.

454 In view of our initial conditions,

455

456 $\left(\frac{\partial K_r}{\partial t}\right)_0 = \left(\frac{\partial K_{rz}}{\partial t}\right)_0 = 0$ (25)

457

458 Thus, as pointed out, earlier our initial conditions are such that the first derivative of perturbation
 459 kinetic energy is made equal to zero. So we have to consider the second derivative of perturbation
 460 kinetic energy K_r , in order to find out the initial change of kinetic energy, then

461

462 $\frac{\partial^2}{\partial t^2} K_{rz} = -\pi \int_0^D U \left[\left(\frac{\partial A}{\partial t}\right)_0 \frac{\partial^2 B_o}{\partial y^2} - B_o \frac{\partial^2}{\partial y^2} \left(\frac{\partial A}{\partial t}\right)_0 \right] dy$ (26)

463

464 Initial conditions are used to get (26)

465

466 Now, we will study the stability properties of different zonal currents with initial disturbance

467

468

469 $\psi = a \sin(ly) \cos(kx)$, i.e., $B_o = a \sin(ly)$ and $A_o = 0$ (27)

470

471 The actual forms of the zonal current will be selected in such a way as to study different aspects of
 472 the problem.

473 (i) the zonal current U is given by

474

475 $U = c \cos(2ly)$ Where $l = \frac{\pi}{D}$

476

477 We shall discuss this symmetric mean zonal current. This profile has two inflection points (where
 478 $\frac{\partial^2 u}{\partial y^2} = 0$) midway between the axis of the flow and the walls. Kuo (1949) found that the presence of
 479 flex points plays an important role in the barotropic stability problem.

480

481 We now need to solve equation (4) for the above prescribed zonal wind profile and B_o (given by
 482 equation 27). β is given as

483

$$484 \quad \beta = \frac{2\Omega \cos(\phi)}{R} = \frac{\Omega}{R} (1 + \cos(2\phi))^{1/2} = \frac{\Omega}{R} (1 + \alpha \cos(ly)) \quad (28)$$

485

486 where R is the radius of the earth and $\alpha < 1$,

487 With the prescribed expressions for U , B and β , equation (4) is solved with the boundary conditions
 488 (7) to give

489

$$490 \quad \left(\frac{\partial A}{\partial t} \right)_o = \frac{-E}{k^2 + l^2} \sin(ly) - \frac{F}{k^2 + 4l^2} \sin(2ly) - \frac{G}{k^2 + 9l^2} \sin(3ly) \dots \quad (29)$$

491

492 Where

$$493 \quad E = \frac{ka\Omega}{R} + \frac{k^3 ac}{2} - \frac{3kacl^2}{2}$$

494

$$495 \quad F = \frac{ka\Omega\alpha}{2R}$$

496

$$497 \quad G = \frac{3}{2} l^2 kac - \frac{k^3 ac}{2}$$

498

499 with the expressions for $\left(\frac{\partial A}{\partial t} \right)_o$, B_o and U , the integral in (26) is evaluated to give

500

501

$$502 \quad \left(\frac{\partial^2 K_r}{\partial t^2} \right)_o = \frac{ka^2 c^2 l^2 \pi D}{k^2 + 9l^2} (3l^2 - k^2) \quad (30)$$

503

504

505

506 $\left(\frac{\partial^2 K_r}{\partial t^2}\right)_o = 0 \quad \text{when } L = \frac{2D}{\sqrt{3}}$ (31)

507

508

509 $> 0 \quad \text{when } L > \frac{2D}{\sqrt{3}}$

510

511

512 $< 0 \quad \text{when } L < \frac{2D}{\sqrt{3}}$

513

514

515

516 *Thus, the neutral wavelength $L < \frac{2D}{\sqrt{3}}$ separates the stable shorter waves and unstable longer waves.*

517 It is to be noted that the terms due to earth's rotation will not appear in (30). So earth's rotation will

518 not contribute to $\left(\frac{\partial^2 K_r}{\partial t^2}\right)_o$ with the symmetric profile for U considered. $\left(\frac{\partial^2 K_r}{\partial t^2}\right)_o$ is maximum at a

519 wavelength 2.1 D and so is the most unstable disturbance.

520

521

522

523

524

525

526

527

528 **References**

529

530 Aihara, M., 1959: Stability properties of large-scale baroclinic disturbances in a vertically and
 531 horizontally variable zonal current. *Journal of Meteorological Society of Japan* **37**, 45-58.

532 Alexander G., Keshavamurty R., De U., Chellappa R., Das S., Pillai P., 1978: Fluctuations of
 533 monsoon activity, *J Meteorol Hydrol Geophys* **29**:76-87

534 Blanford H F. 1886: Rainfall of India. Mem. *India Meteorol. Dep.* **2**:217-448

535 Boos W. R., Hurley J. V., Murthy V. S., 2015: Adiabatic westward drift of Indian monsoon
 536 depressions. *Q. J. R. Meteorol. Soc.* **141**: 1035–1048, doi: 10.1002/qj.2454.

537 Chen W., Yang S., Huang R. H., 2005: Relationship between stationary planetary wave activity and
 538 the East Asian winter monsoon. *Journal of Geophysical Research* **110**: D14110,
 539 DOI:10.1029/2004JD005669

540 Choudhury A., Krishnan R., 2011: Dynamical response of the south Asian monsoon trough to latent
 541 heating from stratiform and convective precipitation, *J Atmos Sci*, **68**:1347–1363

542 Das P. K., 2002: The monsoons. *National Book Trust of India, New Delhi*, **254** pp

543 Goswami, B. N., R. N. Keshavamurthy, and V. Satyan, 1980: Role of barotropic-baroclinic
 544 instability for the growth of monsoon depressions and mid-tropospheric cyclones, *Proc. Indian
 545 Acad. Sci. Earth Planet. Sci.*, **89**, 79 – 97.

546 Goswami, B. N., and R. S. Ajayamohan, 2001: Intra-seasonal oscillations and inter-annual
 547 variability of the Indian summer monsoon, *J. Clim.*, **14**, 1180 – 1198.

548 Goswami, B. N., R. S. Ajayamohan, P. K. Xavier, and D. Sengupta, 2003: Clustering of low
 549 pressure systems during the Indian summer monsoon by intraseasonal oscillations, *Geophys. Res.
 550 Lett.*, **30(8)**, 1431, doi:10.1029/2002GL016734.

551 Goswami, B. N., 2011: South Asian summer monsoon. Intraseasonal Variability in the Atmosphere-
 552 Ocean Climate System. 2nd ed. W. K.-M. Lau and D. E. Waliser, Eds., *Springer*, **21–72**.

553 Hartmann, D. L., and M. L. Michelson, 1989: Intra-seasonal periodicities in Indian rainfall, *J.*
554 *Atmos. Sci.*, **46**, 2838 – 2862.

555 Holton J. R., 2004: An introduction to dynamic meteorology. fourth edition. *Academic Press*,
556 535pp.

557 Joseph S, Sahai AK, Goswami BN. 2009.: Eastward propagating MJO during boreal summer and
558 Indian monsoon droughts. *Clim. Dyn.* **32**: 1139–1153, doi: [10.1007/s00382-008-0412-8](https://doi.org/10.1007/s00382-008-0412-8).

559 Joseph, P.V., Sijikumar, S., 2004: Intraseasonal variability of the low-level jet stream of the
560 Asian summer monsoon. *J. Clim.* **17**, 1449–1458.

561 Kanamitsu, M, Ebisuzaki, W., Woollen J., Yang S-K., Hnilo J.J., Fiorino M., and Potter G. L.,
562 NCEP-DOE AMIP-II Reanalysis (R-2), Nov 2002, *Bulletin of the American Meteorological*
563 *Society*.1631-1643

564 Koteswaram, P., 1958: The easterly jet stream in the tropics. *Tellus* **10**(1): 43–57, DOI
565 DOI:[10.1111/j.2153-3490.1958.tb01984.x](https://doi.org/10.1111/j.2153-3490.1958.tb01984.x)

566 Krishnamurty V., and Ajaymohan R. S., 2010: Composite Structure of Monsoon Low Pressure
567 Systems and its Relation to Indian Rainfall, *J. Clim.*, doi: [10.1175/2010JCLI2953.1](https://doi.org/10.1175/2010JCLI2953.1).

568 Krishnamurthy, V. and J. Shukla, 2000: Intra-seasonal and inter-annual variability of rainfall over
569 India, *J. Clim.*, **13**, 4366-4377.

570 Krishnamurti, T. N., and P. Ardynay, 1980: The 10 to 20 day westward propagating mode and
571 ‘breaks’ in the monsoons, *Tellus*, **32**, 15–26.

572 Krishnamurti, T. N., Stefanova, L., Misra, V., 2013: Tropical meteorology an introduction. Fourth
573 edition, *Springer atmospheric sciences*.DOI [10.1007/978-1-4614-7409-8](https://doi.org/10.1007/978-1-4614-7409-8)

574 Krishnamurthy, V., Shukla, J., 2007: Intraseasonal and seasonally persisting patterns of
575 Indian monsoon rainfall. *J. Clim.* **20**, 3–20.

576 Krishnan R., Zhang C., Sugi M., 2000: Dynamics of breaks in the Indian summer monsoon. *J*
577 *Atmos Sci* **57**:1354–1372

578 Krishnan R., Kumar V., Sugi M., Yoshimura J., 2009: Internal feedbacks from monsoon–mid-

579 latitude interactions during droughts in the Indian summer monsoon, *J Atmos Sci*, **66**:553–578

580 Krishnamurti, T.N. , Subrahmanyam, D., 1982: The 30–50 day mode at 850mb during

581 MONEX. *J. Atmos. Sci.* **39**, 2088–2095.

582 Kuo, H. L., 1953: On the production of mean zonal currents in the atmosphere by large scale

583 disturbances. *Tellus*, **5**, 475-493.

584 Sikka, D. R., and S. Gadgil, 1980: On the maximum cloud zone and the ITCZ over Indian longitude

585 during southwest monsoon, *Mon. Wea. Rev.*, **108**, 1840–1853.

586 Murakami, T., T. Nakazawa, and J. He, 1984: On the 40 – 50 day oscillation during 1979 Northern

587 Hemisphere summer. part I: Phase propagation, *J. Meteorol. Soc. Jpn.*, **62**, 440 – 468.

588 Murakami, T., L. X. Chen, and A. Xie, 1986: Relationship among seasonal cycles, low-frequency

589 oscillations, and transient disturbances as revealed from outgoing long wave radiation data, *Mon.*

590 *Weather Rev.*, **114**, 11,456 – 11,465.

591 Pai, D.S., Bhate, J., Sreejith, O.P., Hatwar, H.R., 2009: Impact of MJO on the intraseasonal

592 variation of summer monsoon rainfall over India. *Clim. Dyn.* doi.org/10.

593 1007/s00382-009-0634-4

594 Raghavan, K., 1973a: Tibetan anticyclone and tropical easterly jet. *Pure Appl Geophys*, **110**:2130–

595 2142

596 Rajeevan M., J. Bhate, J. D. Kale, B. Lal, 2006: High resolution daily gridded rainfall data for the

597 Indian region: analysis of break and active monsoon spells. *Curr Sci* **91**:296–306.

598 Rajeevan, M., S. Gadgil, J. Bhate, 2008: Active and break spells of Indian summer monsoon.

599 *National Climate Centre Research Report No. 7/2008, India Meteorological Department, Pune*,

600 **44** pp. <http://www.imdpune.gov.in>

601 Rajeevan M., Gadgil S., Bhate J., 2010: Active and break spells of the Indian summer monsoon. *J*

602 *Earth Syst Sci*, **119**:229–248

603 Raman, C. R. V., and Y. P. Rao, 1981: Blocking highs over Asia and monsoon droughts over India.

604 *Nature*, **289**, 271–273.

605 Ramamurthy K., 1969: Monsoon of India: some aspects of the 'break' in the Indian southwest
 606 monsoon during July and August. Forecasting Manual, *India Meteorological Department 1-57 No.*

607 **IV 18.3**

608 Ramaswamy C., 1956: The Indian southwest monsoon. Paper read at the Seminar in the
 609 *International Meteorological Institute, Stockholm, Sweden*

610 Ramaswamy C., 1962: Breaks in the Indian summer monsoon as a phenomenon of interaction
 611 between the easterly and the subtropical westerly jet streams. *Tellus* **14**:337–349

612 Rao V.B, 1971: Dynamic instability of the zonal current during a break monsoon, *Tellus* **XXIII**.

613 Rao Y.P., 1976: Southwest monsoon (meteorological monograph). *India Meteorological*
 614 *Department, New Delhi*, **366** pp

615 Sathiyamoorthy, V., P. K. Pal, P. C. Joshi, 2007: Intraseasonal variability of the Tropical Easterly
 616 *Jet. Meteorology and Atmospheric Physics* **96(3-4)**: 305–316, DOI 10.1007/s00703-006-0214-7

617 Satyan V., Keshavamurthy R. N., Goswami B. N., Dash S. K., and Sinha H. S. S., 1980: Monsoon
 618 Cyclogenesis and Large-scale Flow Patterns over South Asia, *Proc. A of Ind. Aca. Sci.* **89**, 79–97

619 Shukla, J., 1978: CISK-barotropic-baroclinic instability and the growth of monsoon depressions. *J.*
 620 *Atmos. Sci.*, **35**, 495-508.

621 Shukla , J., 1987: Interannual variability of monsoon, *Monsoons*, edited by J. S.Fein and P. L.
 622 Stephens, pp. 399 – 464, *John Wiley and Sons, New York*.

623 Sikka D.R., Dixit C.M., 1972: A study of satellite observed cloudiness over the equatorial Indian
 624 ocean and India during the Southwest monsoon season. *J. Mar. Biol. Assoc. India*. **14**:805–18

625 Sikka, D.R., Gadgil, S., 1980: On the maximum cloud zone and the ITCZ over India longitude
 626 during the southwest monsoon. *Mon. Weather Rev.* **108**, 1840–1853.

627 Sikka D. R., Narsimha R., 1995: Genesis of the monsoon trough boundary layer experiment
 628 (MONTBLEX). *Proc Indian Acad Sci* **104**:157–187

629 Singh, S.V., R. H. Kripalani and D. R. Sikka, 1992: Interannual variability of the Madden-Julian
 630 Oscillations in Indian summer monsoon rainfall, *J. Climate*, **5**, 973-979.

631 Starr, V. P., and R. M. White, 1954: Balance requirement of the general circulation. *Geophys.Res.*
 632 *Papers*, **35**, Geophys. Res. Directorate, AFORO.

633 Syono, S., and M. Aihara, 1957: Some characteristic features of barotropic disturbances. *Journal of*
 634 *meteorological society of Japan* **35**, 56-64.

635 Tracks of cyclones and depressions over North Indian Ocean 1891-2015, *Indian Meteorological*
 636 *Department*, Regional Meteorological Centre, Chennai. <http://www.rmcchennaieatlas.tn.nic.in>

637 Waliser, D. E., 2006: Intraseasonal variability. The Asian Monsoon, B. Wang, Ed., *Springer*, **203**–
 638 **258**

639 Yasunari, T., 1981: Structure of an Indian summer monsoon system with around 40-day period, *J.*
 640 *Meteorol. Soc. Jpn.*, **59**, 336 – 354.

641

642

643

644

645 **Tables**

646 **Table 1:** A complete list of the symbols/notations representing various variables/parameters in the
 647 study.

| Symbol | Definition |
|-----------|----------------------|
| U | Zonal wind |
| V | Meridional wind |
| D/2 | Latitudinal distance |
| L_c | Critical wavelength |
| \bar{K} | Mean Kinetic energy |
| K' | Eddy Kinetic energy |
| ζ | Absolute vorticity |
| f | Coriolis force |

| | |
|----|----------------------|
| m | mass |
| u' | eddy zonal wind |
| v' | eddy meridional wind |

648

649

650

651 **Table 2:** Gives the formation of a synoptic disturbance on the particular day after every break event
 652 during the 1979-2007 period. '***' represents the revival of ISM without low formation.

653

| Year | Low formation day after every break event | Condition |
|------|--|---------------|
| 1979 | | *** |
| 1979 | | *** |
| 1980 | 23 July | Bay of Bengal |
| 1980 | 26 August | Bay of Bengal |
| 1981 | | *** |
| 1982 | 19 July | Bay of Bengal |
| 1983 | 4 August | Bay of Bengal |
| 1984 | 30 July | Bay of Bengal |
| 1985 | 28 August | Bay of Bengal |
| 1986 | 9 September | Bay of Bengal |
| 1987 | 11 August | Land Region |
| 1987 | 19 August | Bay of Bengal |
| 1988 | | *** |
| 1989 | 2 August | Bay of Bengal |

| | | |
|------|--------------|---------------|
| 1989 | 16 August | Bay of Bengal |
| 1992 | 18 July | Land Region |
| 1993 | | *** |
| 1993 | | *** |
| 1993 | 6 September | Bay of Bengal |
| 1995 | | *** |
| 1995 | | *** |
| 1996 | | *** |
| 1997 | 22 July | Bay of Bengal |
| 1997 | 16 August | Bay of Bengal |
| 1998 | 1 September | Land Region |
| 1998 | 29 July | Land Region |
| 1999 | | *** |
| 1999 | | *** |
| 1999 | | *** |
| 2000 | 10 August | Bay of Bengal |
| 2001 | 6 August | Bay of Bengal |
| 2001 | 11 September | Land Region |
| 2002 | | *** |
| 2002 | 1 August | Bay of Bengal |
| 2004 | | *** |
| 2004 | 26 July | Land Region |
| 2004 | | *** |
| 2005 | 11 September | Bay of Bengal |
| 2005 | 19 August | Land Region |
| 2007 | | *** |

| | | |
|------|-----------|---------------|
| 2007 | 18 August | Bay of Bengal |
|------|-----------|---------------|

654

655

656

657

658

659 **Table 3:** Conversion of Mean Kinetic Energy Values (Joule/second) at 200 hPa.

660

661

| Year | Before | During | After |
|------|--------------|--------------|--------------|
| | break period | break period | break period |
| 1979 | -533.85 | -324.67 | 568.11 |
| 1979 | -307.49 | -1668.31 | -1040.26 |
| 1980 | -902.14 | 419.32 | -483.19 |
| 1980 | -168.76 | 838.84 | 1241.05 |
| 1981 | -445.01 | 41.06 | 654.83 |
| 1982 | -206.31 | -104.81 | -873.12 |
| 1983 | -483.50 | 932.99 | 345.91 |
| 1984 | -381.30 | 386.58 | -334.05 |
| 1985 | -691.33 | 1736.20 | 864.34 |
| 1986 | -391.23 | 667.50 | 533.51 |
| 1987 | -845.24 | -15.09 | 1909.51 |
| 1987 | -845.24 | 266.40 | -92.27 |
| 1988 | -267.84 | -600.93 | 884.11 |
| 1989 | -134.70 | 1450.52 | 1326.88 |

| | | | |
|------|----------|----------|----------|
| 1989 | -272.84 | 722.94 | -289.01 |
| 1992 | -209.65 | 551.18 | 796.84 |
| 1993 | -662.03 | 641.99 | 500.70 |
| 1993 | -27.15 | -134.37 | 132.38 |
| 1993 | -154.66 | 171.96 | 1059.52 |
| 1995 | -645.48 | 627.13 | -336.83 |
| 1995 | -155.81 | 1094.81 | -499.51 |
| 1996 | -410.98 | 1179.61 | 18.84 |
| 1997 | -348.92 | -435.35 | -1599.46 |
| 1997 | -424.11 | -249.73 | 147.87 |
| 1998 | -111.57 | 296.10 | 1457.89 |
| 1998 | -496.43 | 597.56 | -211.52 |
| 1999 | -409.16 | -320.18 | 178.70 |
| 1999 | -671.99 | 1026.46 | 727.02 |
| 1999 | -691.03 | 1662.09 | 646.58 |
| 2000 | -51.00 | 447.82 | -588.90 |
| 2001 | -547.99 | -1176.18 | -147.23 |
| 2001 | -348.58 | 224.42 | -108.66 |
| 2002 | -1218.62 | 357.86 | -950.32 |
| 2002 | -1218.62 | 818.58 | -950.32 |
| 2004 | -309.27 | 1192.99 | -520.30 |
| 2004 | -309.27 | 558.93 | -520.30 |
| 2004 | -442.18 | 462.54 | 952.01 |
| 2005 | -88.06 | 188.81 | 754.90 |
| 2005 | -418.94 | -341.93 | -275.85 |
| 2007 | -763.64 | 693.70 | 231.90 |

| | | | |
|------|---------|---------|---------|
| 2007 | -384.59 | 1507.19 | 1175.04 |
|------|---------|---------|---------|

662

663

664

665

666

667 **Table 4:** The channel width (D/2) between the subtropical westerly jet and tropical easterly jet (In
 668 degrees) at 200 hPa during the 1979-2007 period.

669

670

| Year | Before break period | During break period | After break period |
|------|------------------------|------------------------|-----------------------|
| 1979 | 35.43 | 28.25 | 26.11 |
| 1979 | 31.00 | 30.00 | 34.50 |
| 1980 | 42.25 | 37.25 | 34.83 |
| 1980 | 28.88 | 23.67 | 31.83 |
| 1981 | 35.00 | 31.75 | 34.29 |
| 1982 | 29.88 | 25.63 | 34.43 |
| 1983 | 33.29 | 35.33 | 36.38 |
| 1984 | 30.63 | 22.67 | 43.00 |
| 1985 | 31.00 | 20.00 | 36.14 |
| 1986 | 33.57 | 26.00 | 26.25 |
| 1987 | 26.10 | 29.83 | 22.67 |
| 1987 | 32.14 | 29.33 | 39.14 |
| 1988 | 38.00 | 32.75 | 30.83 |

| | | | |
|------|-------|-------|-------|
| 1989 | 26.43 | 28.00 | 43.29 |
| 1989 | 48.86 | 40.20 | 44.00 |
| 1992 | 31.22 | 28.88 | 39.63 |
| 1993 | 30.43 | 25.75 | 42.43 |
| 1993 | 33.86 | 22.29 | 31.43 |
| 1993 | 30.14 | 28.57 | 38.43 |
| 1995 | 34.57 | 26.80 | 37.71 |
| 1995 | 35.29 | 28.67 | 37.83 |
| 1996 | 37.38 | 39.00 | 37.83 |
| 1997 | 41.71 | 39.20 | 34.29 |
| 1997 | 34.43 | 30.83 | 41.00 |
| 1998 | 29.00 | 23.00 | 30.67 |
| 1998 | 24.29 | 23.14 | 35.43 |
| 1999 | 24.43 | 25.80 | 26.14 |
| 1999 | 39.57 | 35.80 | 25.86 |
| 1999 | 31.43 | 20.50 | 39.43 |
| 2000 | 34.63 | 28.89 | 37.33 |
| 2001 | 25.43 | 26.33 | 37.43 |
| 2001 | 34.00 | 29.40 | 29.57 |
| 2002 | 29.86 | 31.43 | 38.86 |
| 2002 | 29.86 | 30.82 | 38.86 |
| 2004 | 28.13 | 32.25 | 40.20 |
| 2004 | 28.13 | 23.67 | 40.2 |
| 2004 | 29.70 | 23.33 | 31.00 |
| 2005 | 31.86 | 24.25 | 38.63 |
| 2005 | 32.71 | 33.63 | 34.86 |

| | | | |
|------|-------|-------|-------|
| 2007 | 25.38 | 25.20 | 29.43 |
| 2007 | 37.57 | 37.00 | 40.57 |

671

672

673

674

675 **Table 5:** Calculated values of wavelength (L_c Km) before, during and after break periods.

676

677

| Year | Before | During | After |
|------|--------------|--------------|--------------|
| | break period | break period | break period |
| 1979 | 9082 | 7310 | 6693 |
| 1979 | 7947 | 7690 | 8844 |
| 1980 | 10831 | 9549 | 8929 |
| 1980 | 7402 | 6067 | 8160 |
| 1981 | 8972 | 8139 | 8789 |
| 1982 | 7658 | 6569 | 8826 |
| 1983 | 8533 | 9057 | 9324 |
| 1984 | 7851 | 5810 | 11023 |
| 1985 | 7947 | 5127 | 9265 |
| 1986 | 8606 | 6665 | 6729 |
| 1987 | 6691 | 7648 | 5810 |
| 1987 | 8240 | 7519 | 10034 |
| 1988 | 9741 | 8395 | 7904 |
| 1989 | 6775 | 7178 | 11096 |

| | | | |
|------|-------|-------|-------|
| 1989 | 12524 | 10305 | 11279 |
| 1992 | 8004 | 7402 | 10158 |
| 1993 | 7800 | 6601 | 10876 |
| 1993 | 8679 | 5713 | 8057 |
| 1993 | 7727 | 7324 | 9851 |
| 1995 | 8862 | 6870 | 9668 |
| 1995 | 9045 | 7349 | 9698 |
| 1996 | 9581 | 9997 | 9698 |
| 1997 | 10693 | 10049 | 8789 |
| 1997 | 8826 | 7904 | 10510 |
| 1998 | 7434 | 5896 | 7861 |
| 1998 | 6225 | 5933 | 9082 |
| 1999 | 6262 | 6614 | 6702 |
| 1999 | 10144 | 9177 | 6628 |
| 1999 | 8057 | 5255 | 10107 |
| 2000 | 8876 | 7405 | 9570 |
| 2001 | 6518 | 6750 | 9595 |
| 2001 | 8716 | 7536 | 7580 |
| 2002 | 7654 | 8057 | 9961 |
| 2002 | 7654 | 7900 | 9961 |
| 2004 | 7210 | 8267 | 10305 |
| 2004 | 7210 | 6067 | 10305 |
| 2004 | 7613 | 5981 | 7947 |
| 2005 | 8166 | 6216 | 9901 |
| 2005 | 8386 | 8620 | 8935 |
| 2007 | 6505 | 6460 | 7544 |

| | | | |
|------|------|------|-------|
| 2007 | 9631 | 9485 | 10400 |
|------|------|------|-------|

678

679 **Table A1:** A complete list of the symbols/notations representing various variables/parameters in
 680 the appendix.

681

682

683

| Symbol | Definition |
|------------------------------------|--|
| f | Coriolis parameter |
| ϕ | Latitude |
| $\boldsymbol{v}_E = \nabla^2 \psi$ | Relative vorticity |
| ψ | Stream function for perturbation flow |
| u | Zonal wind |
| v | Meridional wind |
| U | Mean zonal wind |
| $\beta = \frac{df}{dy}$ | Rossby factor |
| $k = \frac{2\pi}{L}$ | Wave number |
| t | time |
| L | Wavelength |
| D | Channel width |
| Q | Any disturbance quantity |
| A, B | Amplitude |
| K_r | Perturbation Kinetic energy |
| K_{r_z} | Zonal kinetic energy |
| R | Radius of Earth |
| | Incremental zonal & meridional distances |

| | |
|-----------------|--|
| dx & dy | used in integration/differentiation |
| a, α , c | Wavelength |
| Ω | Vertical 'p' velocity |
| ω | Angular speed of the earth |
| Δ | Del operator applied to a quantity which varies on an isobaric surface |
| Δ^2 | Laplacian operator |

684
685

686

687

688

689

690 **Figures**

691

692 Figure 1.

693 Observed Sea Level Pressure (SLP) distribution, after the break period (10 Aug, 2000).

694

695 Figure 2.

696 Conversion of Kinetic Energy anomaly values for the 1979-2007 period.

697 Figure 3.

698 (a) Observed U- wind at 200hpa on 4august, 2000, a typical break day (b) the corresponding

699 Geopotential distribution (in Km).

700 Figure 4.

701 (a) Eddy momentum flux transfer during (1-9 August), before (14-23 July) and after (10-15 August)

702 break periods of a break event in the year 2000. (b) Zonal wind at 200hpa during (4th August),703 before (23rd July) and after (11th August) break periods of a break event in the year 2000.

704 Figure 5.

705 Composite of absolute vorticity profiles of break spells for the period of 1979-2007. (b) Multiple
706 plot of absolute vorticity profiles of break periods.

707 Figure 6.

708 Latitudinal distance between westerlies and easterlies of the zonal wind at 200 hPa of the break
709 events of each monsoon season.

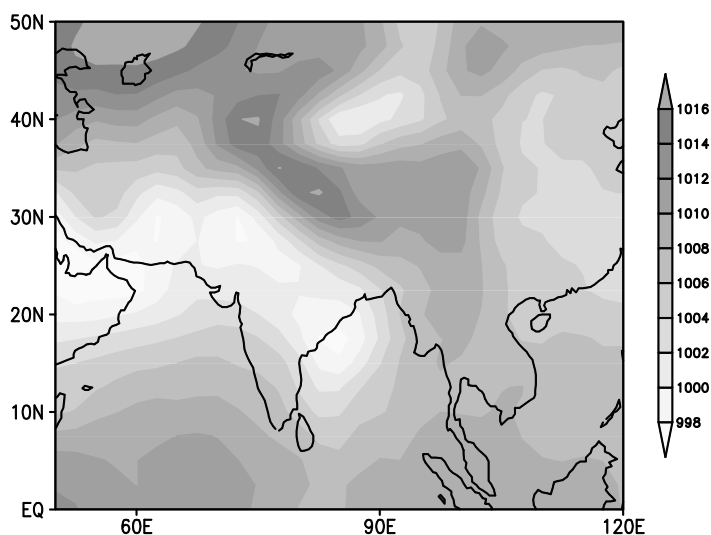
710 Figure 7.

711 Wavelength anomalies of the zonal wind at 200 hPa averaged over the break events of each
712 monsoon season.

713

714

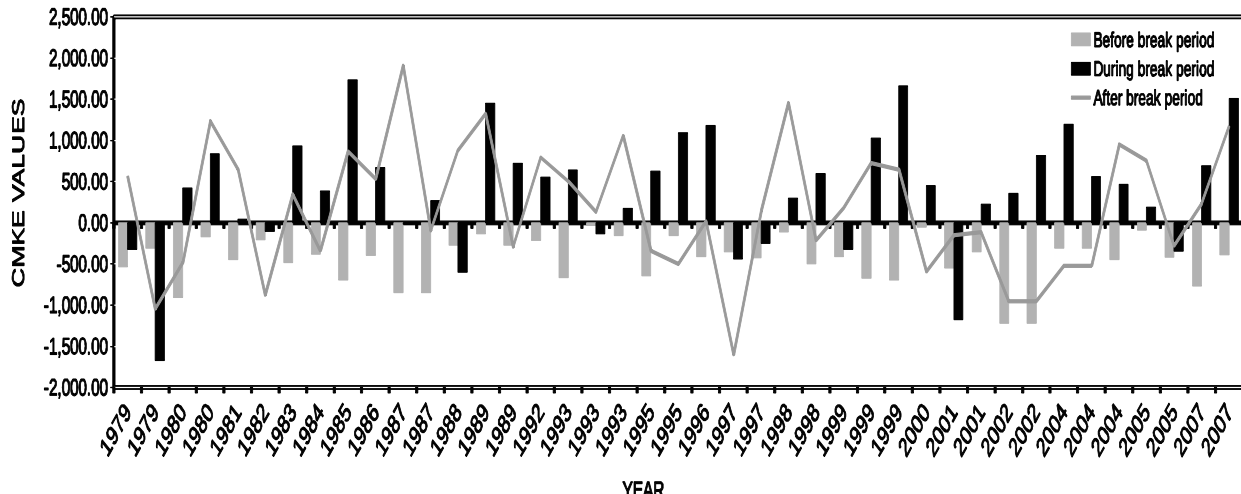
715



716

717 1. Observed Sea Level Pressure (SLP) distribution, after the break period (10 Aug, 2000).

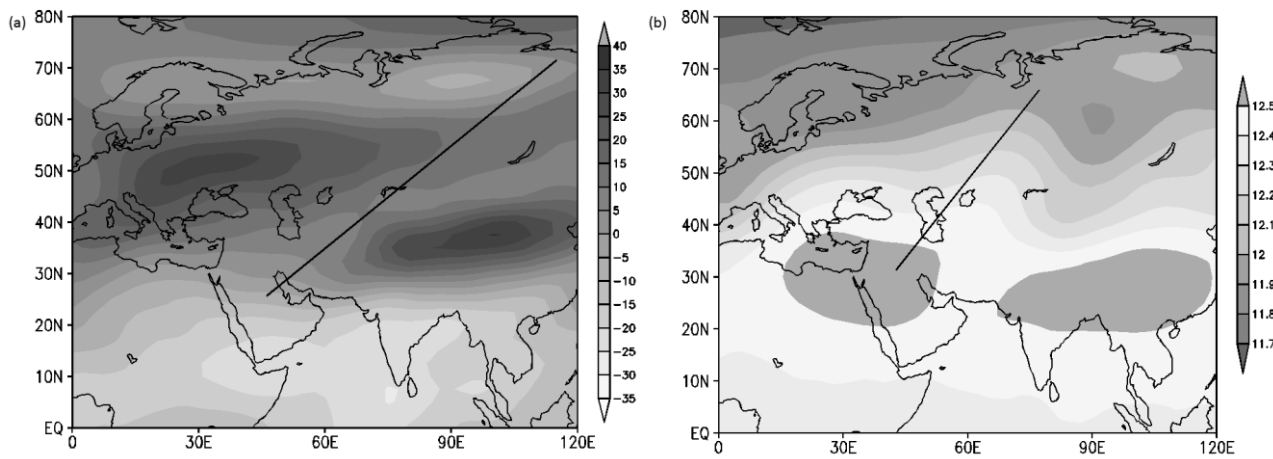
718



719

720 2. Conversion of Kinetic Energy (J/s) anomaly values for the 1979-2007 period.

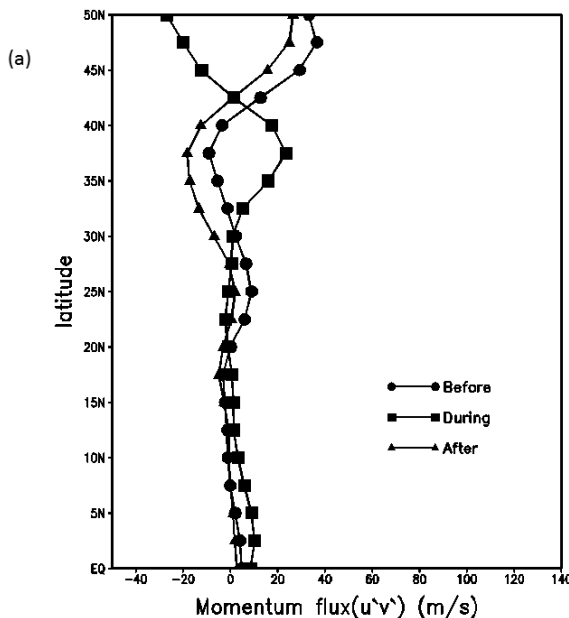
721



722

723

724 3. (a) Observed U-wind at 200hpa on 4 august, 2000, a typical break day (b) the
 725 corresponding Geopotential distribution (in Km).



726

727

728

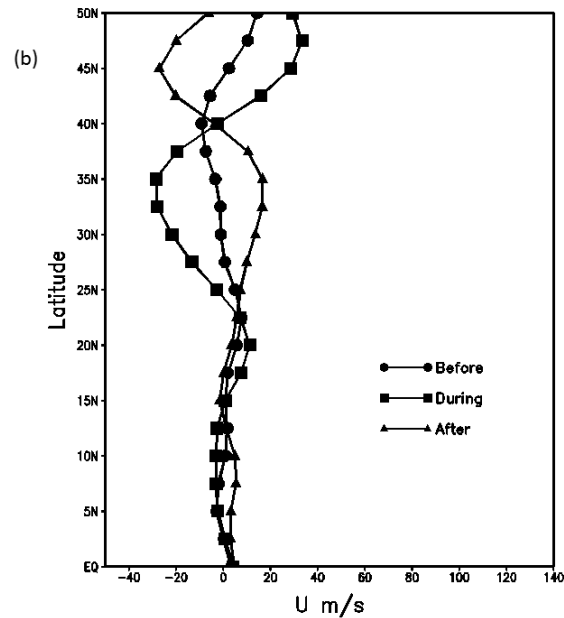
729

730

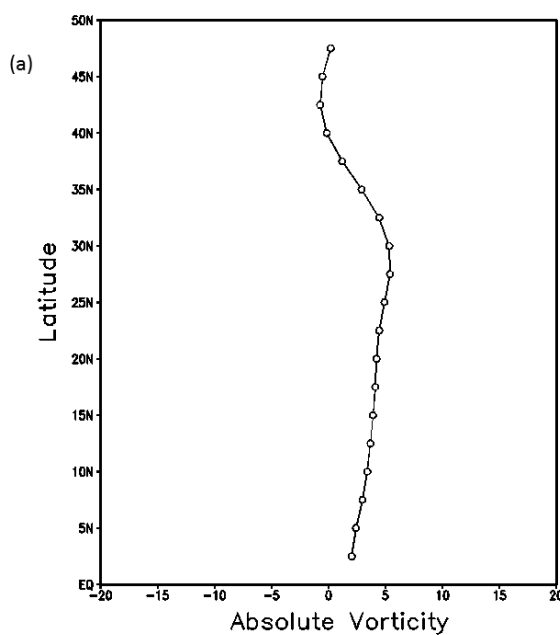
731

732

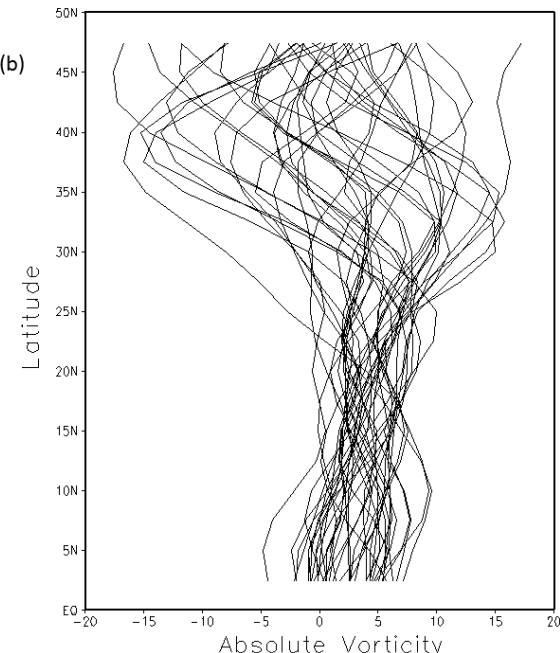
733



4. (a) Eddy momentum flux transfer during (1-9 August), before (14-23 July) and after (10-15 August) break periods of a break event in the year 2000. (b) Zonal wind structure of a typical break event at 200hpa, during (4th August), before (23rd July) and after (11th August) break periods in the year 2000.



734



735

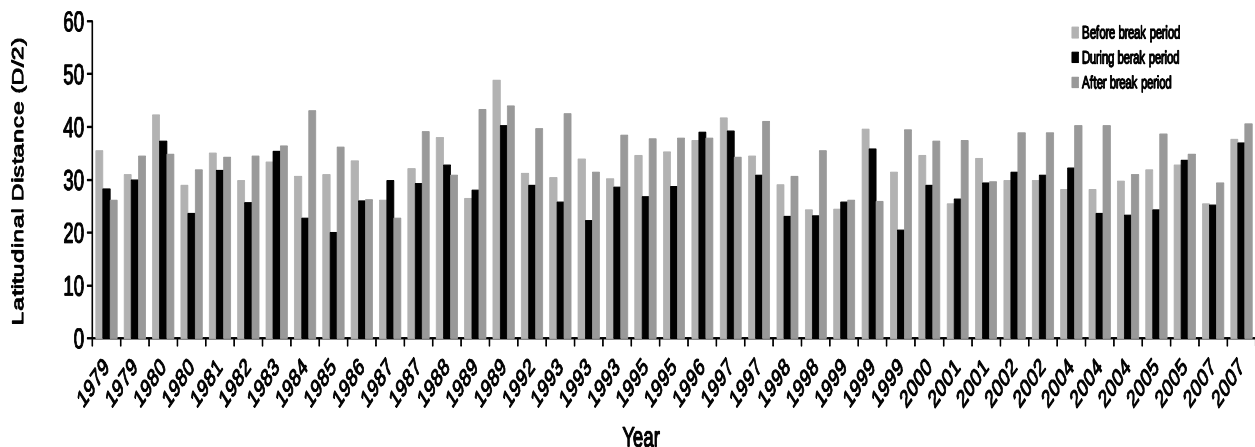
736

737 5. (a) Composite of absolute vorticity profiles of break spells for the period of 1979-2007.

738 (b) Multiple plot of absolute vorticity profiles of all 41 break periods.

739

740

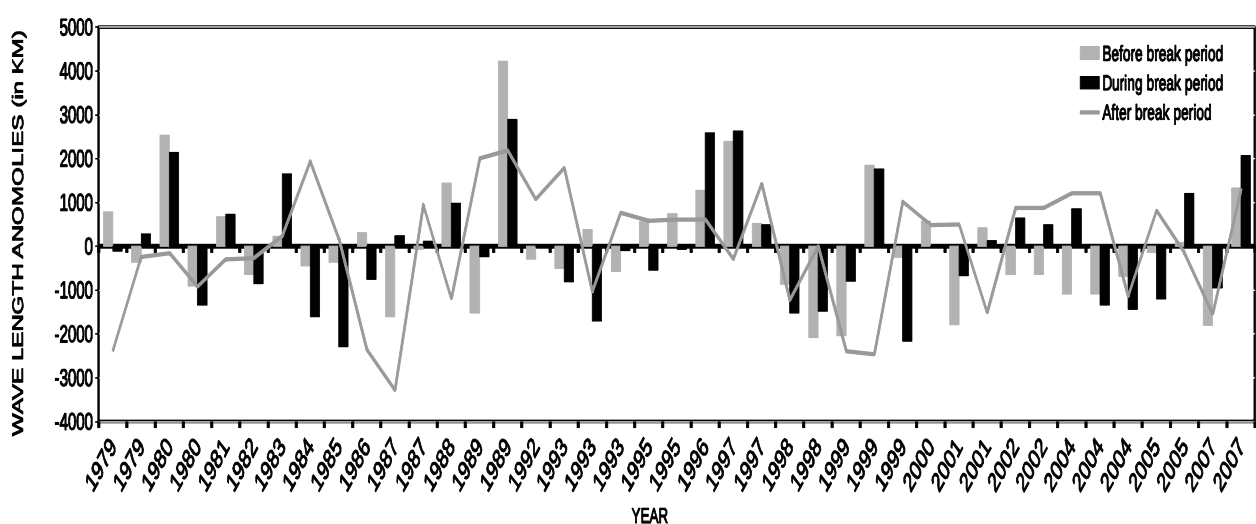


741

742 6. Latitudinal distance (in degrees) between westerlies and easterlies of the zonal wind at
743 200 hPa of the break events of each monsoon season.

744

745



746

747 7. Wavelength anomalies of the zonal wind at 200 hPa averaged over the break events of
748 each monsoon season.